Biology of Human Primary Bone Marrow Mesenchymal Stromal Stem Cells

Ghazanfari, Roshanak

2017

Stem Cell Reports
Report
OPEN ACCESS

Low/Negative Expression of PDGFR-α Identifies the Candidate Primary Mesenchymal Stromal Cells in Adult Human Bone Marrow

Hongzhe Li,[1] Roshanak Ghazanfari,[1] Dimitra Zacharaki,[1] Nicholas Ditzel,[2] Joan Isern,[3] Marja Ekblom,[1,6] Simón Méndez-Ferrer,[3] Moustapha Kassem,[2,4,5] and Stefan Scheding[1,6,*]

[1]Lund Stem Cell Center, Lund University, 22184 Lund, Sweden
[2]Department of Endocrinology, University of Southern Denmark, Molecular Endocrinology Laboratory (KMEB), Odense 5000, Denmark
[3]Centro Nacional de Investigaciones Cardiovasculares Carlos III, Madrid 28029, Spain
[4]Stem Cell Unit, College of Medicine, King Saud University, Riyadh 11461, Saudi Arabia
[5]Danish Stem Cell Center (DanStem), Panum Institute, University of Copenhagen, Copenhagen 2200, Denmark
[6]Department of Hematology, Skåne University Hospital Lund, 22184 Lund, Sweden
*Correspondence: stefan.scheding@med.lu.se
http://dx.doi.org/10.1016/j.stemcr.2014.09.018

SUMMARY

Human bone marrow (BM) contains a rare population of nonhematopoietic mesenchymal stromal cells (MSCs), which are of central importance for the hematopoietic microenvironment. However, the precise phenotypic definition of these cells in adult BM has not yet been reported. In this study, we show that low/negative expression of CD140a (PDGFR-α) on lin$^-$/CD45$^-$/CD271$^+$ BM cells identified a cell population with very high MSC activity, measured as fibroblastic colony-forming unit frequency and typical in vitro and in vivo stroma formation and differentiation capacities. Furthermore, these cells exhibited high levels of genes associated with mesenchymal lineages and HSC supportive function. Moreover, lin$^-$/CD45$^-$/CD271$^+$/CD140a$^{low/-}$ cells effectively mediated the ex vivo expansion of transplantable CD34$^+$ hematopoietic stem cells. Taken together, these data indicate that CD140a is a key negative selection marker for adult human BM-MSCs, which enables to prospectively isolate a close to pure population of candidate human adult stroma stem/progenitor cells with potent hematopoiesis-supporting capacity.

INTRODUCTION

Human bone marrow (BM) contains—besides the well-known hematopoietic stem cells (HSCs)—a population of nonhematopoietic mesenchymal stromal cells (MSCs), which are multipotent and can differentiate toward skeletal lineages in vivo (Sacchetti et al., 2007). In vitro, clonogenic cells, which are denoted as colony-forming unit-fibroblasts (CFU-Fs) (Friedenstein et al., 1970), can be assayed from the BM as plastic adherent cells giving rise to fibroblastic colonies. These CFU-F cells are considered to reflect the primary BM-MSC, and upon further proliferation in culture, their descendants make up the extensively studied cultured MSCs (Keating, 2012).

BM-MSCs are able to generate hematopoietic stroma upon transplantation in vivo, thus providing the specialized microenvironments for HSCs (Sacchetti et al., 2007). Furthermore, BM-MSCs have been shown to play an important role in regulating self-renewal and differentiation of HSCs (Méndez-Ferrer et al., 2010), and they have also been implicated in the development of hematological malignancies (Raaijmakers et al., 2010).

However, the precise in vivo identity and phenotypic signature of adult BM-MSCs have thus far remained elusive (Keating, 2012). Therefore, this current study aimed for a precise phenotypic characterization of the human BM stromal cell population by utilizing comparative gene expression profiling as a screening tool. Based on this screening, low/negative expression of CD140a (PDGFR-α) was identified as the key feature that enabled the isolation of a close to pure population of primary MSC in adult human BM nonhematopoietic CD271$^+$ cells. In contrast, human fetal BM-MSCs were recently reported to be CD140a positive (Pinho et al., 2013), indicating that PDGFR-α expression is regulated developmentally.

RESULTS AND DISCUSSION

Comparative Gene Expression Analysis of lin$^-$/CD45$^-$/CD271$^+$ versus lin$^-$/CD45$^-$/CD271$^-$ BM Cells Identifies Human MSC Markers

We and others have shown that CFU-Fs were highly and exclusively enriched only in lin$^-$/CD45$^-$/CD271$^+$ BM cells but not in the CD271$^-$ fraction (Churchman et al., 2012; Tormin et al., 2011). Therefore, an array-based gene expression analysis was performed comparing these two cell populations as a screening tool to identify potential MSC surface markers (the sorting strategy is presented in Figure S1 available online). In total, 219 genes were significantly upregulated in the CD271$^+$ subset, including typical MSC genes as well as genes encoding for cytokines, growth factors, and extracellular matrix proteins (Table S1).

Twenty-eight upregulated genes were related to surface-expressed molecules (Figure 1A; Table S2). Only eight genes were cell surface markers that had been previously reported

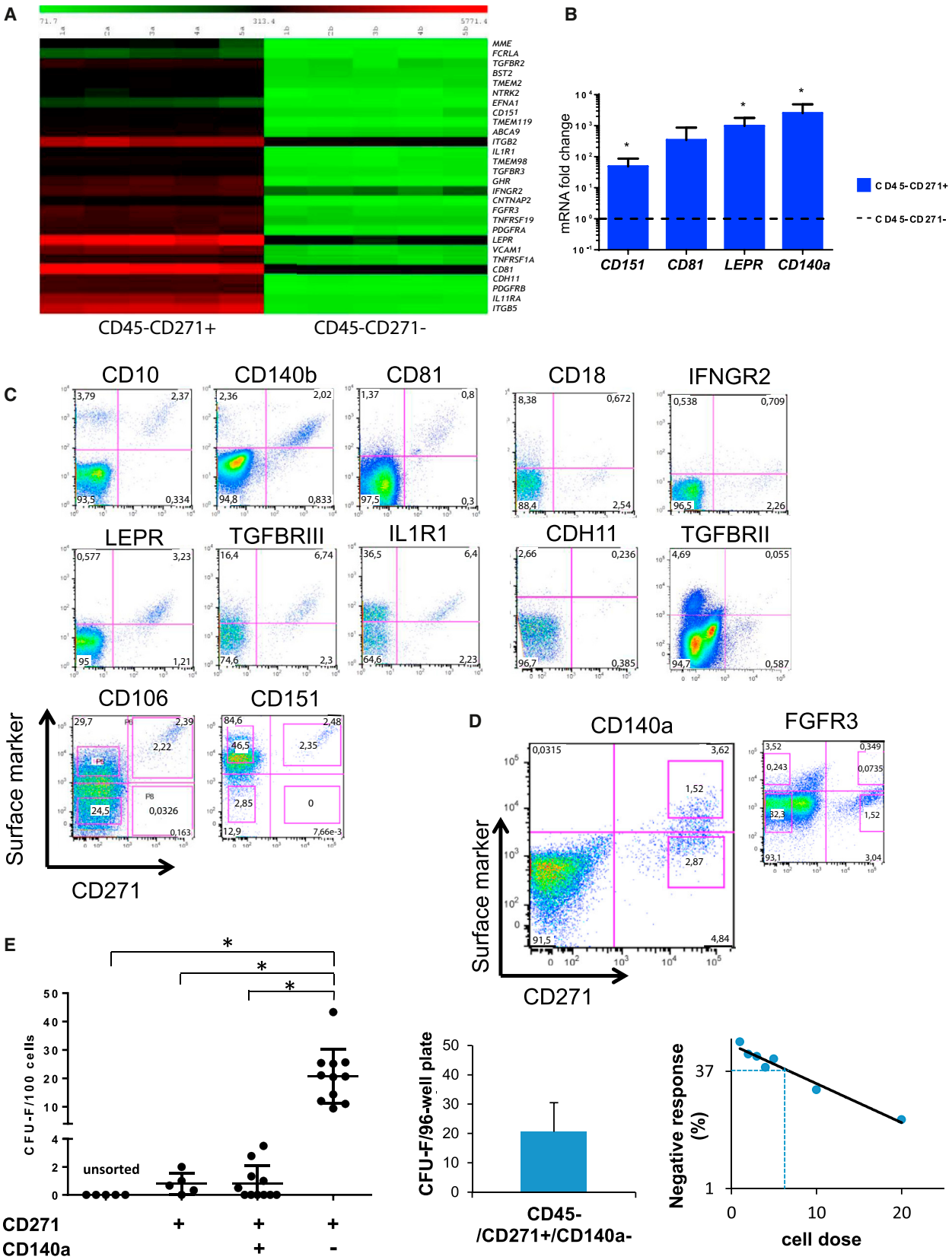

(legend on next page)

to be expressed on primary MSCs, i.e., LEPR/CD295, TGFBRIII, CDH11, and FGFRIII (Churchman et al., 2012); CD140b, CD10, CD106 (Battula et al., 2008; Bühring et al., 2007; Gronthos et al., 2003); and CD140a (Pinho et al., 2013). The remaining 20 genes, of which four were selected for validation by quantitative RT-PCR confirming the results of the gene array (Figure 1B), had not been reported in the context of MSC isolation.

Cell-Surface Expression Analysis of Potential MSC Markers on lin$^-$/CD45$^-$/CD271$^+$ Cells

Next, protein expression was validated for those candidate surface markers for which antibodies were commercially available. Lin$^-$/CD45$^-$/CD271$^+$ cells expressed high levels of CD10, CD140b, CD81, leptin receptor (LEPR), transforming growth factor beta receptor III (TGFBRIII), interleukin 1 receptor alpha (IL1R1), CD106, and CD151, while expression of CD18, interferon gamma receptor 2 (IFNGR2), cadherin-11 (CDH11), transforming growth factor beta receptor II (TGFBRII), CD140a, and fibroblast growth factor receptor 3 (FGFR3) was low/intermediate (Figures 1C and 1D). TNFR1 was the only candidate gene for which measurable protein expression levels were not detected (data not shown).

Most of the identified markers showed a staining pattern that paralleled CD271 expression; i.e., expression levels of the newly discovered marker increased with increasing CD271 levels (group I markers; Figure 1C). Therefore, these markers would not be expected to improve CFU-F enrichment in sorted CD271$^+$ cells. Accordingly, experiments using CD151 as an example (Figure 1C, lower panel), demonstrated that CFU-F frequencies were not significantly different compared with isolation based on CD271 and other known MSC markers, such as CD106 (Figure 1C, lower panel; Figure S2A). As expected, sorted lin$^-$/CD45$^-$/CD271$^+$/CD151$^+$ cells showed all typical MSC properties in vitro (Figures S2A–S2F) and in vivo, i.e., formation of human MSC-derived bone, stroma invaded by murine hematopoietic cells, and an increase in vessel density (Figures S2G–S2I). LEPR is another group I marker that was recently reported to identify the majority of CFU-F in adult murine BM (Zhou et al., 2014). Our data showed that LEPR expression is conserved; i.e., that the majority of human adult CFU-F is contained in the LEPR$^+$ fraction (Figure S2J).

Group II Marker CD140a, but Not FGFR3, Allows Isolation of a Close to Pure Population of CFU-F-Initiating Cells

On the other hand, CD140a and FGFR3 (group II markers) showed a more orthogonal staining pattern, allowing us to identify subpopulations of CD140a$^+$, CD140a$^{low/-}$ and FGFR3$^+$, FGFR3$^{low/-}$ cells, respectively (Figure 1D).

Whereas sorting based on FGFR3 expression did not improve CFU-F enrichment (data not shown), very high CFU-F frequencies were observed when CD271$^+$ cells were sorted according to low/negative CD140a expression (Figure 1E). Mean CFU-F frequencies in bulk cultures seeded at clonal densities were as high as 20.8 ± 9.6 CFU-F per 100 cells in the CD140a$^{low/-}$ fraction compared with 0.8 ± 1.2 CFU-F per 100 plated CD140a$^+$ cells and 0.8 ± 0.8 CFU-F per 100 plated CD271$^+$ cells (Figure 1E, left graph). Similar results were obtained by single cell assays and limiting dilution analysis (Figure 1E, middle and right graphs, respectively). Considering that the high frequency of progenitor activity corresponds well to that reported for other immunophenotypically defined stem cell populations, such as HSCs, lin$^-$/CD45$^-$/CD271$^+$/CD140a$^{low/-}$ cells are likely to represent a (close to) pure population of primary MSCs in human adult BM.

Recently, Mabuchi et al., (2013) reported comparable CFU-F frequencies by using a direct two-marker isolation approach (CD271, CD90). However, experiments in their study were performed with femoral bone fragments, which contain only few hematopoietic cells. In contrast,

Figure 1. Gene Expression Analysis Identifies MSC Surface Markers of which CD140a Enables Isolation of a Highly Enriched CFU-F Population

(A) Heatmap of significantly upregulated surface molecule genes in lin$^-$/CD45$^-$/CD271$^+$ versus lin$^-$/CD45$^-$/CD271$^-$ cells of five donors.
(B) Quantitative RT-PCR of lin$^-$/CD45$^-$/CD271$^-$ compared with CD271$^+$ cells. Results are shown as mRNA fold change after standardizing with *GAPDH* levels. Data are from three individual experiments with duplicate measurements for each of the genes. *$p < 0.05$.
(C and D) Lineage depleted BM-MNCs were stained with antibodies as indicated and analyzed by flow cytometry. Representative plots of CD271 expression (x axis) versus expression of the indicated marker (y axis) are shown after forward-scatter/side-scatter gating, exclusion of dead cells (7-AAD), and gating on CD45-negative cells. Sorting gates are indicated in the CD106, CD151 (C), and CD140a and FGFR3 plots (D).
(E) CFU-F frequencies of primary lin$^-$/CD45$^-$/CD271$^+$ BM cell populations sorted on CD140a expression. Data are presented as individual data (dots) from bulk sorting (left plot, n = 5–11 independent experiments with at least three replicates for each experiment), and three independent limiting dilution experiments with seven different cell concentrations for each experiment (right plot, each dot in the plot represents the average of the three experiments). Single cell sorting data were calculated from three independent experiment, and data are given as mean ± SD (middle plot). The sorting strategy is illustrated in Figure S3. *$p < 0.05$.
See also Figures S1 and S2 and Tables S1, S2, and S3.

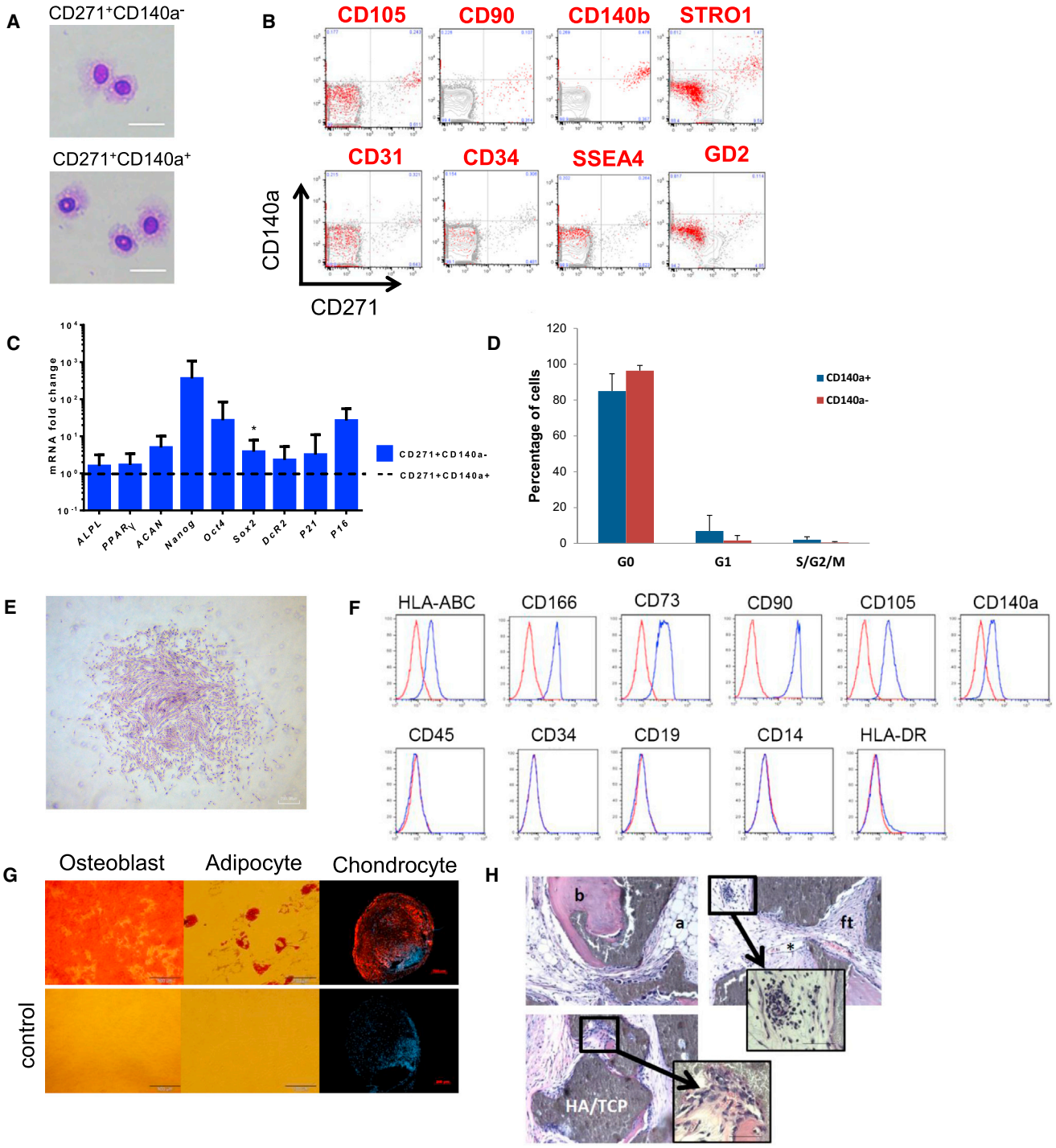

Figure 2. Properties of Primary and Cultured CD45$^-$/CD271$^+$/CD140a$^{low/-}$ Cells

(A) Cytospin preparations of CD45$^-$/CD271$^+$/CD140a$^{low/-}$ and CD45$^-$/CD271$^+$/CD140a$^+$ cells (May-Grünwald/Giemsa staining). Scale bars represent 20 μm.

(B) FACS analysis of primary lin$^-$/CD45$^-$ BM-MNC. Events are plotted for CD271 (x axis) against CD140a (y axis) expression. Red events indicate cells that coexpressed the marker listed on top, i.e., CD105, CD90, CD140b, STRO-1, CD31, CD34, SSEA4, and CD34, respectively, whereas gray events indicate lack of coexpression. One representative set of FACS plots of a total of three experiments is shown.

(legend continued on next page)

hematopoietically active BM as used in our study contains CD90$^+$ hematopoietic cells, and CFU-F activity is also detected in CD90$^-$ cells (data not shown), which indicates that the CD271/CD90 two-marker approach is not suitable to enrich CFU-F from standard BM aspirations.

Primary lin$^-$/CD45$^-$/CD271$^+$/CD140a$^{low/-}$ Cells Exhibit a Typical BM-MSC Phenotype and Give Rise to Typical Cultured MSCs

Cytospin preparations of lin$^-$/CD45$^-$/CD271$^+$/CD140a$^{low/-}$ and CD140a$^+$ cells showed a typical MSC morphology with cytoplasmic vacuoles and large, immature nuclei (Figure 2A). Furthermore, lin$^-$/CD45$^-$/CD271$^+$/CD140a$^{low/-}$ cells expressed signature MSC markers, such as CD90, CD105, CD140b, and STRO-1 while lacking expression of CD31, CD34 (Figure 2B). As reported previously (Tormin et al., 2011), SSEA-4 and GD2 were not detected on primary BM-MSCs (Figure 2B), which might be due to differences in experimental protocols. Among lin$^-$/CD45$^-$/CD271$^+$ cells, expression of pluripotency genes (*Nanog*, *Oct4*, *Sox2*) and cyclin-dependent kinase inhibitor gene *p16* was higher in CD140a$^{low/-}$ than in CD140a$^+$ cells (Figure 2C). Comparable gene expression was observed for differentiation genes (*ALPL*, *PPARγ*, *ACAN*), *p21*, and decoy receptor 2 (*DCR2*). Furthermore, short-term differentiation induction experiments (24 hr) increased expression of *PPARγ* and *ACAN* only in CD140a$^{low/-}$ MSCs but not in CD140$^+$ cells (data not shown). Cell cycle distributions of CD140a$^+$ and CD140a$^{low/-}$ cells were not significantly different, but a trend was observed toward more quiescent CD140a$^-$ cells (Figure 2D). These data indicate that CD140a$^{low/-}$ MSCs represent a distinct population of immature, quiescent stem/progenitor cells with multilineage potential.

Stromal cell cultures generated from sorted lin$^-$/CD45$^-$/CD271$^+$/CD140a$^{low/-}$ cells (single-cell as well as bulk) were composed of typical adherent, spindle-shaped, fibroblastic-like cells (Figure 2E), with a typical MSC surface marker profile (Figure 2F). Interestingly, CD140a expression increased in culture, which might be influenced by cell attachment, cell density, and culture medium composition. Lin$^-$/CD45$^-$/CD271$^+$/CD140a$^+$ cells did not generate sufficient colonies for further studies. In contrast, CD140a$^{low/-}$-derived cultured stromal cells demonstrated robust multilineage differentiation potential in vitro (Figure 2G). This was not only observed in multiclonal cultures from bulk-sorted cells, but also in single-cell-derived clones, of which 62%, 31%, and 7% exhibited trilineage, bilineage, and unilineage differentiation potential, respectively. Finally, in vivo differentiation potential was tested by subcutaneous implantation of lin$^-$/CD45$^-$/CD271$^+$/CD140a$^{low/-}$-derived cells into immunodeficient mice. In addition to bone, adipocytes, and stromal tissues, invading hematopoietic cells were clearly identified in the ectopic scaffolds (Figure 2H). These results thus demonstrate that CD140a$^{low/-}$ cells have the capacity to generate hematopoietic stroma in vivo, a key property of primary BM-MSCs (Sacchetti et al., 2007).

Hematopoiesis-Supporting Capacity of lin$^-$/CD45$^-$/CD271$^+$/CD140a$^{low/-}$ Cells

We have recently shown that primitive BM-MSCs promote the ex vivo expansion of human umbilical cord blood (CB)-derived CD34$^+$ cells (Isern et al., 2013). These results prompted us to assess the hematopoiesis-supporting capacity of lin$^-$/CD45$^-$/CD271$^+$/CD140a$^{low/-}$ cells in coculture assays with CB CD34$^+$ cells. CD34$^+$ hematopoietic cells were evenly distributed and in close contact with the feeder cells only when cocultured with the lin$^-$/CD45$^-$/CD271$^+$/CD140a$^{low/-}$ cells and their stromal derived progeny, i.e., cultured mesenchymal stroma cells (cMSCs) (Figures 3A and 3B). CD271$^-$/CD140a$^+$ cells did not form confluent feeder layers, and thus, CD34$^+$ cocultures showed a similar distribution pattern as the nonfeeder cell cultures (Figure 3A).

(C) Quantitative RT-PCR was performed on sorted lin$^-$/CD45$^-$/CD271$^+$/CD140a$^+$ and lin$^-$/CD45$^-$/CD271$^+$/CD140a$^{low/-}$ cells. Results are shown as mRNA fold change after standardizing with *GAPDH* levels. Data are given as mean ± SD. Data are from three to eight individual experiments with duplicate measurements for each of the genes. *$p < 0.05$.
(D) Cell cycle analysis of the CD45$^-$/CD271$^+$/CD140a$^{low/-}$ and CD45$^-$/CD271$^+$/CD140a$^+$ cells by KI67 and DNA staining (n = 3 independent experiments).
(E) Morphology of colonies derived from CD45$^-$/CD271$^+$/CD140a$^{low/-}$ cells (crystal violet staining). Scale bar represents 200 μm.
(F) Flow cytometric analysis of MSC marker expression of CD45$^-$/CD271$^+$/CD140a$^{low/-}$-derived cultured stromal cells (blue line) and corresponding isotype controls (red line). A representative set of data of a total of three experiments is shown.
(G) In vitro differentiation capacity of stromal cells derived from bulk-sorted CD45$^-$/CD271$^+$/CD140a$^{low/-}$ cells toward the osteoblastic, adipogenic, and chondrogenic lineage (upper panel). Controls are shown in the lower panel. Scale bars represent 500 μm (osteoblast), 100 μm (adipocyte), and 200 μm (chondrocyte). A representative set of pictures from a total of three experiments is shown.
(H) Multiclonal cultures generated from CD45$^-$/CD271$^+$/CD140a$^{low/-}$ cells were transplanted subcutaneously (with HA/TCP particles) into NOD/SCID mice. Representative sections 8 weeks after transplantation are shown. Bone (b), adipocytes (a), fibroblastic tissue (ft), and capillaries (*) are indicated (magnification 10×). Blowups are shown at 60× magnification. Invading hematopoietic cells (upper blowup) and megakaryocytes (lower blowup) could be detected. Scale bar represents 20 μm.
See also Figures S3 and S4 and Table S3.

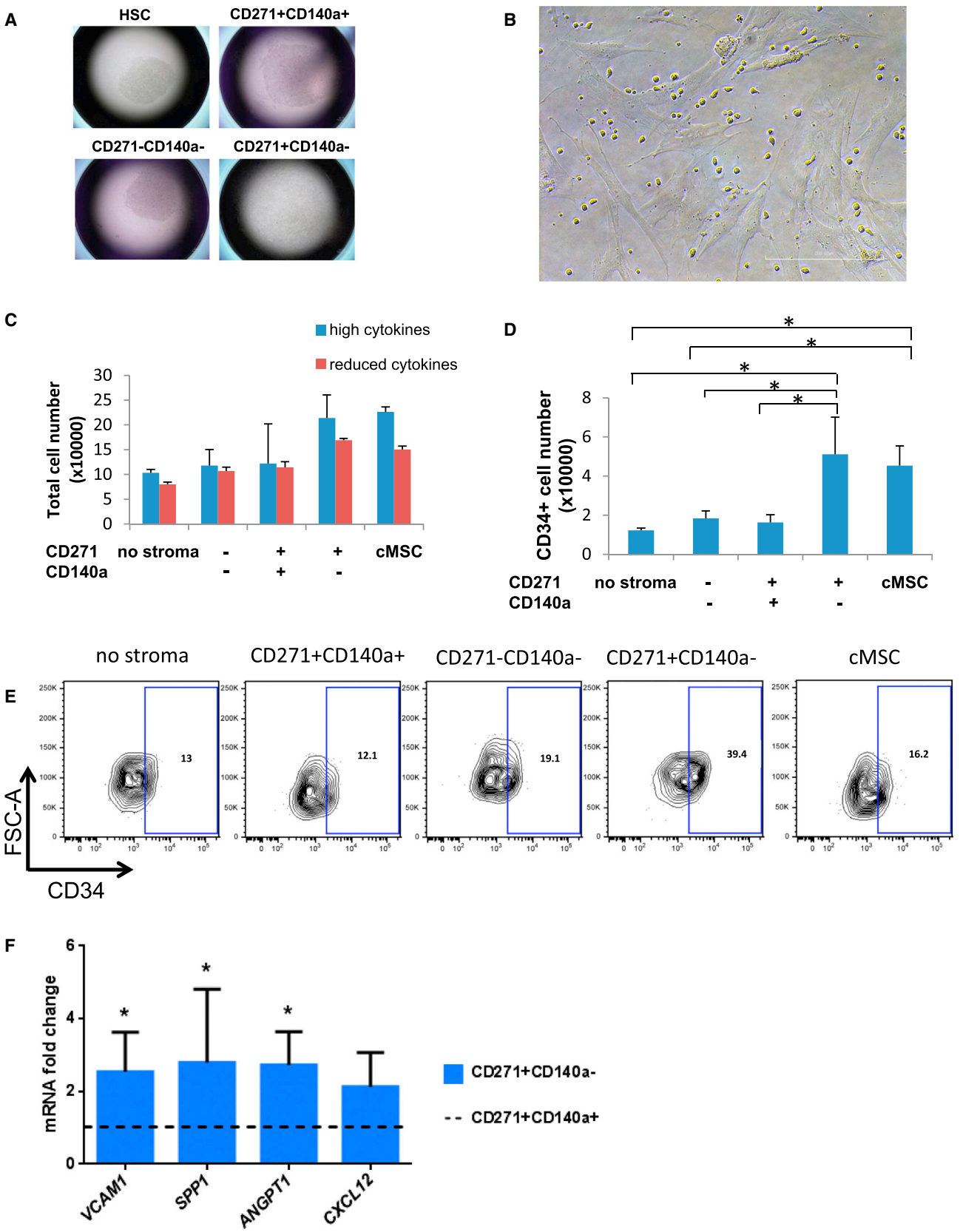

(legend on next page)

One week coculture with lin$^-$/CD45$^-$/CD271$^+$/CD140a$^{low/-}$ cells increased total cell production in cytokine-supported expansion cultures (Figure 3C), which was comparable with cMSC as feeder cells. Moreover, the number of CD34$^+$ cells was the best in lin$^-$/CD45$^-$/CD271$^+$/CD140a$^{low/-}$ supported cultures (Figure 3D), which showed a better preservation of the CD34$^+$ phenotype compared with cMSC (Figure 3E). Correspondingly, lin$^-$/CD45$^-$/CD271$^+$/CD140a$^{low/-}$ cells showed high expression of hematopoiesis-supporting genes (*VCAM1*, *SPP1*, *CXCL12*, and *angiopoietin 1*; Figure 3F). CD34$^+$ cells expanded on lin$^-$/CD45$^-$/CD271$^+$/CD140a$^{low/-}$ feeder cells or cMSCs were capable of efficient long-term hematopoietic multilineage reconstitution in immunodeficient mice (Figure 4).

CD140a, which is a long-known marker for murine MSCs, has only recently been reported as a positive marker to identify human fetal BM CFU-F-initiating cells (Pinho et al., 2013). However, adult BM cells are by far the most commonly used MSC source, and our data clearly demonstrate that MSCs are highly enriched within the CD140a$^{low/-}$ population but not in CD140$^+$ cells. This distribution pattern is also observed in older adults, even though CFU-F frequencies in CD140a$^{low/-}$ cells are lower (Figure S4). On the other hand and consistent with previous work (Pinho et al., 2013), we found that fetal CD140a$^+$ cells had an increased CFU-F frequency, clearly contrasting the results in adult BM cells. These data suggest that CD140a expression is progressively downregulated during development, which was also supported by examination of the CD140a expression of murine BM-MSCs at different developmental stages (Figure S4D).

Platelet-derived growth factor (PDGF) is a key signaling molecule in the complex bone formation process and a powerful mitogen and chemoattractant for MSCs, inducing proliferation as well as affecting directional mobility (Caplan and Correa, 2011). Increased PDGFR-α signaling in embryos leads to hyperplasia of stromal fibroblasts (Olson and Soriano, 2009). The MSC enrichment in the CD140a$^+$ fraction during bone development and its progressive downregulation strongly suggest that it might be required for osteoprogenitor activity possibly also under pathological conditions, but our results suggest that this receptor may not necessarily be essential for the HSC niche function of BM-MSCs.

In summary, based on comparative gene expression analysis, we could demonstrate that low/negative expression of CD140a identified a close to pure population of the putative stromal stem/progenitor cells in human adult BM, which is likely to be a critical first step toward a better functional characterization of these important constituents of the hematopoietic microenvironment.

EXPERIMENTAL PROCEDURES

BM Mononuclear Cells

A total of 111 BM samples were collected from 87 healthy adult donors (median age, 25 years; range 19–41) plus three additional older donors (52, 56, and 61 years). BM (60 ml) was aspirated from the iliac crest bone of consenting healthy donors. BM aspiration was approved by the local ethics committee. BM-MNCs were isolated by density gradient centrifugation (LSM 1077 Lymphocyte; PAA) with or without prior incubation with RosetteSep Human MSC Enrichment Cocktail (StemCell Technologies) for lineage depletion (CD3, CD14, CD19, CD38, CD66b, glycophorin A). The preparation of fetal BM cells is described in Figure S3.

Generation of Cultured MSCs and CFU-F Assays

Sorted BM-MNCs were cultured in standard MSC culture medium (NH Expansion Medium; Miltenyi Biosciences) and passaged as described (Tormin et al., 2011). CFU-F assays were performed as before (Tormin et al., 2011); a detailed description is provided in the Supplemental Experimental Procedures.

Microarray Expression Analysis

RNA from sorted cell populations was isolated, amplified, and analyzed for gene expression microarray analysis using Illumina Human HT-12 expression v4 BeadChips (Illumina). Detailed experimental procedures and data analysis are described in the Supplemental Experimental Procedures.

Figure 3. CD45$^-$/CD271$^+$/CD140a$^{low/-}$ Cells Promote the Ex Vivo Expansion of CB CD34$^+$ Cells

(A) Representative pictures of individual culture wells. HSCs indicate well with CD34$^+$ cells that were cultured without stromal support.

(B) Photomicrograph illustrating CB CD34$^+$ coculture on CD45$^-$/CD271$^+$/CD140a $^{low/-}$ stromal cells. Scale bar represents 200 μm.

(C and D) Total number of hematopoietic cells (C) and CD34$^+$ cells (D) produced after 1-week culture. Data are calculated from three individual experiments and provided as mean ± SD (n = 3). *p < 0.05.

(E) Representative FACS profile of coculture-generated cells.

(F) Quantitative RT-PCR of sorted lin$^-$/CD45$^-$/CD271$^+$/CD140a$^+$ and lin$^-$/CD45$^-$/CD271$^+$/CD140a$^{low/-}$ cells. Results are shown as mRNA fold change after standardizing with *GAPDH* levels. Data are given as mean ± SD. Data are from three individual experiments with duplicate measurements for each of the genes. *p < 0.05.

CB CD34$^+$ cells were cocultured for 1 week with CD45$^-$/CD271$^+$/CD140a$^{low/-}$, CD45$^-$/CD271$^+$/CD140a$^+$, CD45$^-$/CD271$^-$/CD140a$^-$ cells or standard cultured stromal cells (cMSCs). Cultures were supplemented with SCF, TPO, and Flt3L at concentrations of 25 or 100 ng/ml (reduced or high cytokines). See also Table S3.

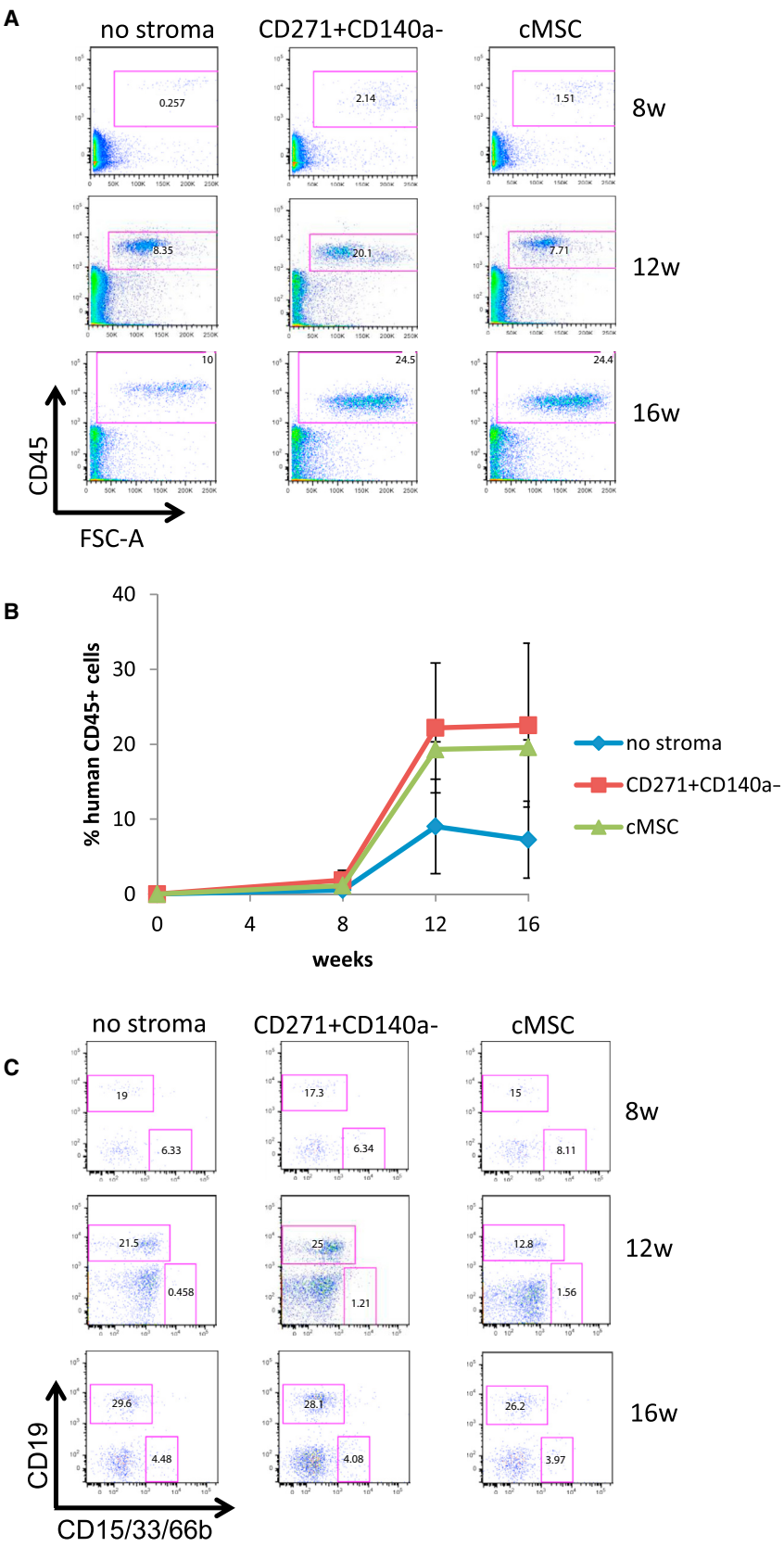

Figure 4. Engraftment Capacity of CB CD34$^+$ Cells Ex Vivo Expanded on CD45$^-$/CD271$^+$/CD140a$^{low/-}$ Feeder Cells

Analysis of human hematopoietic cell engraftment following intravenous transplantation of the culture equivalent of 50,000 input CD34$^+$ cells into NSG mice. CB blood CD34$^+$ cells were cocultured for 1 week with or without feeder cells in cytokine-supplemented medium (SCF, TPO, Flt3L at 25 ng/ml). Engraftment was assessed after 8, 12, and 16 weeks using human-specific CD45 antibodies (A and B) and CD15/CD33/CD66 and CD19 antibodies (C). Representative FACS plots are shown. Data in (B) represent the mean ± SD of a total of four to six mice per time point.

Fluorescence-Activated Cell Sorting

Lineage-depleted BM-MNCs were incubated in blocking buffer (Dulbecco's PBS [DPBS] without Ca^{2+}, Mg^{2+}, 3.3 mg/ml human normal immunoglobulin [Octapharma], 1% fetal bovine serum [Life Technologies]), followed by staining with monoclonal antibodies against CD45, CD151, CD140a, and CD271 (for detailed information on all antibodies used in this study, please see the Supplemental Experimental Procedures). Sorting gates were set according to the corresponding fluorescence-minus-one controls. Cells were sorted on fluorescence-activated cell sorting (FACS) Aria I or FACS Aria III cell sorters (BD Bioscience). Dead cells were excluded by 7-amino-actinomycin staining (7-AAD; Sigma), and doublets were excluded by gating on forward scatter height versus forward scatter width and side scatter height versus side scatter width. Flow cytometry analysis is described in the Supplemental Experimental Procedures.

In Vitro Differentiation Assays

Cultured MSCs were differentiated toward the adipogenic, osteoblastic, and chondrogenic lineages as described previously (Tormin et al., 2011). Briefly, cells were cultured for 14 days in AdipoDiff medium (Miltenyi) and were stained with Oil red O (Sigma). For osteogenic differentiation, cells were cultured in osteogenesis induction medium (see the Supplemental Experimental Procedures) for 21 days and stained with alizarin red (Sigma). Chondrogenic differentiation was induced by culturing cell pellets (2.5×10^5 cells/pellet) for 56 days in chondrogenesis-induction medium (see the Supplemental Experimental Procedures). Cryosections of paraformaldehyde-fixed pellets were stained against aggrecan as described previously (Tormin et al., 2011). Nuclei were stained with 4′,6-diamidino-2-phenylindole (Life Technologies). Sections were analyzed with an Axiovert 200M fluorescence microscope and an AxioCam HRm (both from Carl Zeiss).

Quantitative RT-PCR

RNA from sorted $lin^-/CD45^-/CD271^+/CD140a^{low/-}$ and $lin^-/CD45^-/CD271^+/CD140a^+$ and $lin^-/CD45^-/CD271^+/CD151^+$ populations was isolated from at least three individual donors. cDNA was synthesized and quantitative RT-PCR analysis was performed (for more details and primers, see Supplemental Experimental Procedures and Table S3).

In Vivo Bone and Stroma Assay

For analysis of in vivo bone and stroma formation, cells were culture derived from sorted $CD45^-/CD271^+/CD140a^{low/-}$ and $CD45^-/CD271^+/CD151^+$ cells from three different donors. Cells were loaded overnight on hydroxyapatite/tricalcium phosphate (HA/TCP) ceramic powder and implanted subcutaneously into 8-week-old female nonobese diabetic/severe combined immunodeficiency (NOD/SCID) mice (5×10^5 cells, four implants per culture). Implants were removed after 8 weeks, fixed, decalcified, and paraffin embedded. Sections were stained with hematoxylin/eosin and analyzed as described (Abdallah et al., 2008). All animal procedures were approved by the local ethical committees on animal experiments.

$CD34^+$ Cells Isolation from CB

Umbilical CB samples were obtained from full-term, normal deliveries with informed consent in accordance with institutional guidelines and as approved by the local ethical committee. Isolation and enrichment of $CD34^+$ cells from CB samples were carried out on mononuclear cells by magnetic-activated cells sorting (Miltenyi) according to manufacturer's instructions. Cells were subsequently frozen in freezing buffer (90% fetal calf serum plus 10% DMSO).

Coculture of CB $CD34^+$ Cells with BM-MSCs

Different FACS-sorted primary BM stromal cell populations or culture-derived MSCs (third or fourth passage) were plated into 96-well plates at 1,000 cells per well and cultured in nonhematopoietic medium for 7–10 days. Then medium was removed, and 5,000 CB $CD34^+$ cells were added onto the adherent stromal cells in serum-free expansion medium (StemCell Technologies) supplemented with 25 or 100 ng/ml of stem cell factor (SCF), thrombopoietin (TPO), and FLT3-ligand (FLT3L) (all from Peprotech). Cells were harvested, counted, and analyzed after 1 week of coculture.

In Vivo HSC Repopulation Assay

Eight- to 12-week old female NOD.Cg-*Prkdc*^{scid}*Il2rg*^{tmlWjl}/SzJ (NOD/SCID-IL2Rγ_c null; NSG) mice (Jackson Laboratory) were sublethally irradiated (300 cGy) 24 hr prior to transplantation. CB $CD34^+$ cells were cultured for 1 week in cytokine-supported serum-free medium (25 ng/ml of SCF, TPO, and FLT3L) with or without feeder cells (no cells, short-term cultured $CD45^-/CD271^+/CD140a^{low/-}$ cells, or fourth passage cultured MSCs, respectively). Noncultured CB $CD34^+$ cells served as an additional control. The culture equivalent of 50,000 input $CD34^+$ cells was intravenously injected, and human engraftment was assessed 8, 12, and 16 weeks after transplantation by flow cytometry (human-specific antibodies against CD45, CD15/CD33/CD66b, and CD19). All animal experiments were approved by local animal ethics committee, Lund University.

Statistical Analysis

Data are expressed as mean ± SD. For a comparison of two samples, the two-tailed Student's t test was used. For multiple comparisons, data were analyzed by one-way ANOVA using the Bonferroni post-test. Differences are reported significant when $p < 0.05$.

SUPPLEMENTAL INFORMATION

Supplemental Information includes Supplemental Experimental Procedures, four figures, and three tables and can be found with this article online at http://dx.doi.org/10.1016/j.stemcr.2014.09.018.

ACKNOWLEDGMENTS

This work was supported by funds from the Swedish Research Council (VR), the HematoLinné and StemTherapy Program, the Swedish Cancer Foundation, the Swedish Childhood Cancer Foundation, Gunnar Nilsson's Cancer Foundation, Gunnel Björk's Testament, ALF (Government Public Health Grant), and the Skåne County Council's Research Foundation. The authors thank Helene

Larsson for help with the BM samples and the Lund Stem Cell Center FACS facility for excellent technical assistance.

Received: November 29, 2013
Revised: September 25, 2014
Accepted: September 26, 2014
Published: October 30, 2014

REFERENCES

Abdallah, B.M., Ditzel, N., and Kassem, M. (2008). Assessment of bone formation capacity using in vivo transplantation assays: procedure and tissue analysis. Methods Mol. Biol. *455*, 89–100.

Battula, V.L., Treml, S., Abele, H., and Bühring, H.J. (2008). Prospective isolation and characterization of mesenchymal stem cells from human placenta using a frizzled-9-specific monoclonal antibody. Differentiation *76*, 326–336.

Bühring, H.J., Battula, V.L., Treml, S., Schewe, B., Kanz, L., and Vogel, W. (2007). Novel markers for the prospective isolation of human MSC. Ann. N.Y. Acad. Sci. *1106*, 262–271.

Caplan, A.I., and Correa, D. (2011). PDGF in bone formation and regeneration: new insights into a novel mechanism involving MSCs. J. Orthop. Res. *29*, 1795–1803.

Churchman, S.M., Ponchel, F., Boxall, S.A., Cuthbert, R., Kouroupis, D., Roshdy, T., Giannoudis, P.V., Emery, P., McGonagle, D., and Jones, E.A. (2012). Transcriptional profile of native CD271+ multipotential stromal cells: evidence for multiple fates, with prominent osteogenic and Wnt pathway signaling activity. Arthritis Rheum. *64*, 2632–2643.

Friedenstein, A.J., Chailakhjan, R.K., and Lalykina, K.S. (1970). The development of fibroblast colonies in monolayer cultures of guinea-pig bone marrow and spleen cells. Cell Tissue Kinet. *3*, 393–403.

Gronthos, S., Zannettino, A.C., Hay, S.J., Shi, S., Graves, S.E., Kortesidis, A., and Simmons, P.J. (2003). Molecular and cellular characterisation of highly purified stromal stem cells derived from human bone marrow. J. Cell Sci. *116*, 1827–1835.

Isern, J., Martín-Antonio, B., Ghazanfari, R., Martín, A.M., López, J.A., del Toro, R., Sánchez-Aguilera, A., Arranz, L., Martín-Pérez, D., Suárez-Lledó, M., et al. (2013). Self-renewing human bone marrow mesenspheres promote hematopoietic stem cell expansion. Cell Rep. *3*, 1714–1724.

Keating, A. (2012). Mesenchymal stromal cells: new directions. Cell Stem Cell *10*, 709–716.

Mabuchi, Y., Morikawa, S., Harada, S., Niibe, K., Suzuki, S., Renault-Mihara, F., Houlihan, D.D., Akazawa, C., Okano, H., and Matsuzaki, Y. (2013). LNGFR(+)THY-1(+)VCAM-1(hi+) Cells Reveal Functionally Distinct Subpopulations in Mesenchymal Stem Cells. Stem Cell Rep. *1*, 152–165.

Méndez-Ferrer, S., Michurina, T.V., Ferraro, F., Mazloom, A.R., Macarthur, B.D., Lira, S.A., Scadden, D.T., Ma'ayan, A., Enikolopov, G.N., and Frenette, P.S. (2010). Mesenchymal and haematopoietic stem cells form a unique bone marrow niche. Nature *466*, 829–834.

Olson, L.E., and Soriano, P. (2009). Increased PDGFRalpha activation disrupts connective tissue development and drives systemic fibrosis. Dev. Cell *16*, 303–313.

Pinho, S., Lacombe, J., Hanoun, M., Mizoguchi, T., Bruns, I., Kunisaki, Y., and Frenette, P.S. (2013). PDGFRα and CD51 mark human nestin+ sphere-forming mesenchymal stem cells capable of hematopoietic progenitor cell expansion. J. Exp. Med. *210*, 1351–1367.

Raaijmakers, M.H., Mukherjee, S., Guo, S., Zhang, S., Kobayashi, T., Schoonmaker, J.A., Ebert, B.L., Al-Shahrour, F., Hasserjian, R.P., Scadden, E.O., et al. (2010). Bone progenitor dysfunction induces myelodysplasia and secondary leukaemia. Nature *464*, 852–857.

Sacchetti, B., Funari, A., Michienzi, S., Di Cesare, S., Piersanti, S., Saggio, I., Tagliafico, E., Ferrari, S., Robey, P.G., Riminucci, M., and Bianco, P. (2007). Self-renewing osteoprogenitors in bone marrow sinusoids can organize a hematopoietic microenvironment. Cell *131*, 324–336.

Tormin, A., Li, O., Brune, J.C., Walsh, S., Schütz, B., Ehinger, M., Ditzel, N., Kassem, M., and Scheding, S. (2011). CD146 expression on primary nonhematopoietic bone marrow stem cells is correlated with in situ localization. Blood *117*, 5067–5077.

Zhou, B.O., Yue, R., Murphy, M.M., Peyer, J.G., and Morrison, S.J. (2014). Leptin-receptor-expressing mesenchymal stromal cells represent the main source of bone formed by adult bone marrow. Cell Stem Cell *15*, 154–168.

Stem Cell Reports, Volume *3*

Supplemental Information

Low/Negative Expression of PDGFR-α Identifies the Candidate Primary Mesenchymal Stromal Cells in Adult Human Bone Marrow

Hongzhe Li, Roshanak Ghazanfari, Dimitra Zacharaki, Nicholas Ditzel, Joan Isern, Marja Ekblom, Simón Méndez-Ferrer, Moustapha Kassem, and Stefan Scheding

Figure S1

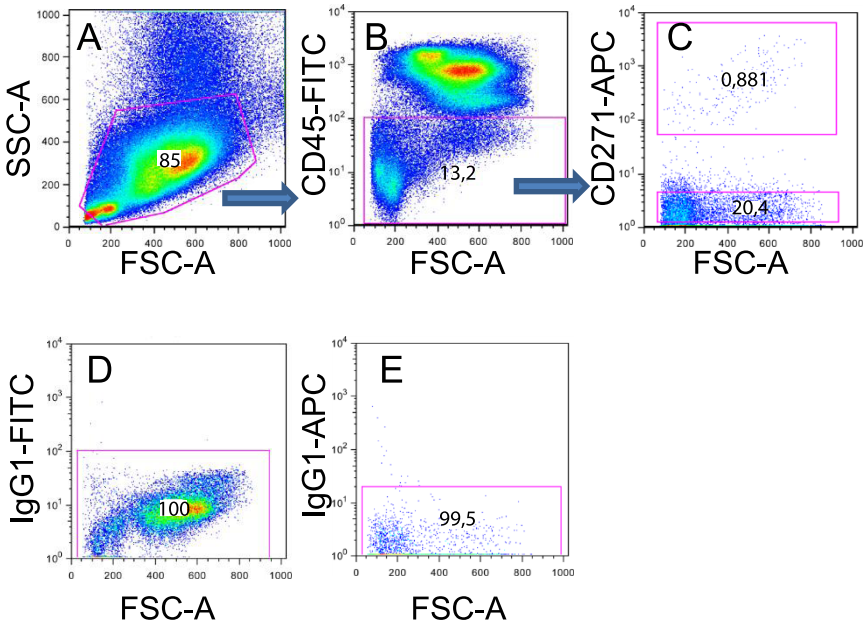
A
SSC-A
FSC-A
85
B
CD45-FITC
FSC-A
13,2
C
CD271-APC
FSC-A
0,881
20,4
D
IgG1-FITC
FSC-A
100
E
IgG1-APC
FSC-A
99,5

Figure S2

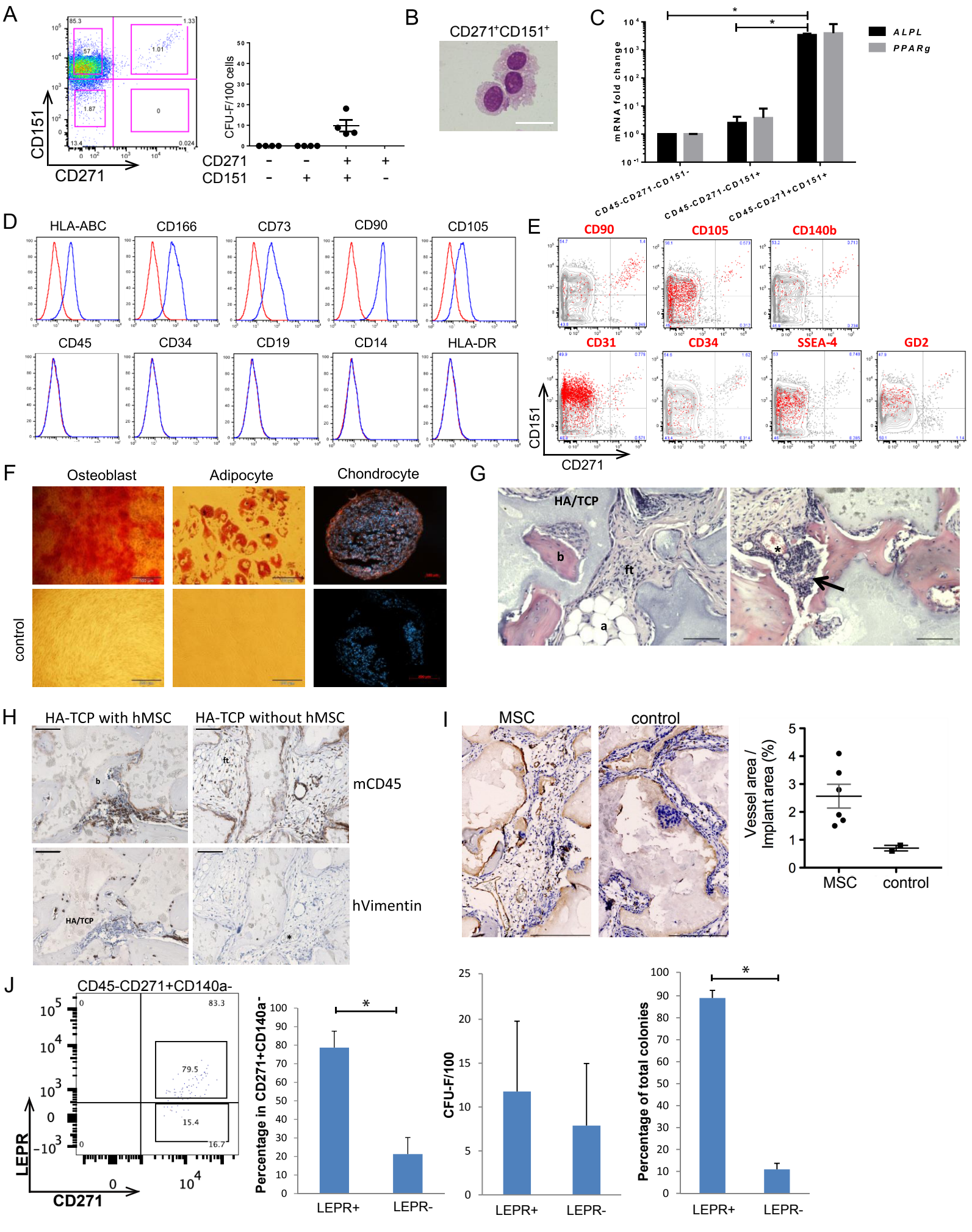
A
CD151
CD271
CFU-F/100 cells
CD271 - - + +
CD151 - + + -
B
CD271+CD151+
C
mRNA fold change
ALPL
PPARg
CD45-CD271-CD151-
CD45-CD271-CD151+
CD45-CD271+CD151+
D
HLA-ABC
CD166
CD73
CD90
CD105
CD45
CD34
CD19
CD14
HLA-DR
E
CD90
CD105
CD140b
CD31
CD34
SSEA-4
GD2
CD151
CD271
F
Osteoblast
Adipocyte
Chondrocyte
control
G
HA/TCP
b
ft
a
*
H
HA-TCP with hMSC
HA-TCP without hMSC
mCD45
hVimentin
HA/TCP
I
MSC
control
Vessel area / Implant area (%)
MSC
control
J
CD45-CD271+CD140a-
LEPR
CD271
Percentage in CD271+CD140a-
LEPR+
LEPR-
CFU-F/100
Percentage of total colonies

Figure S3

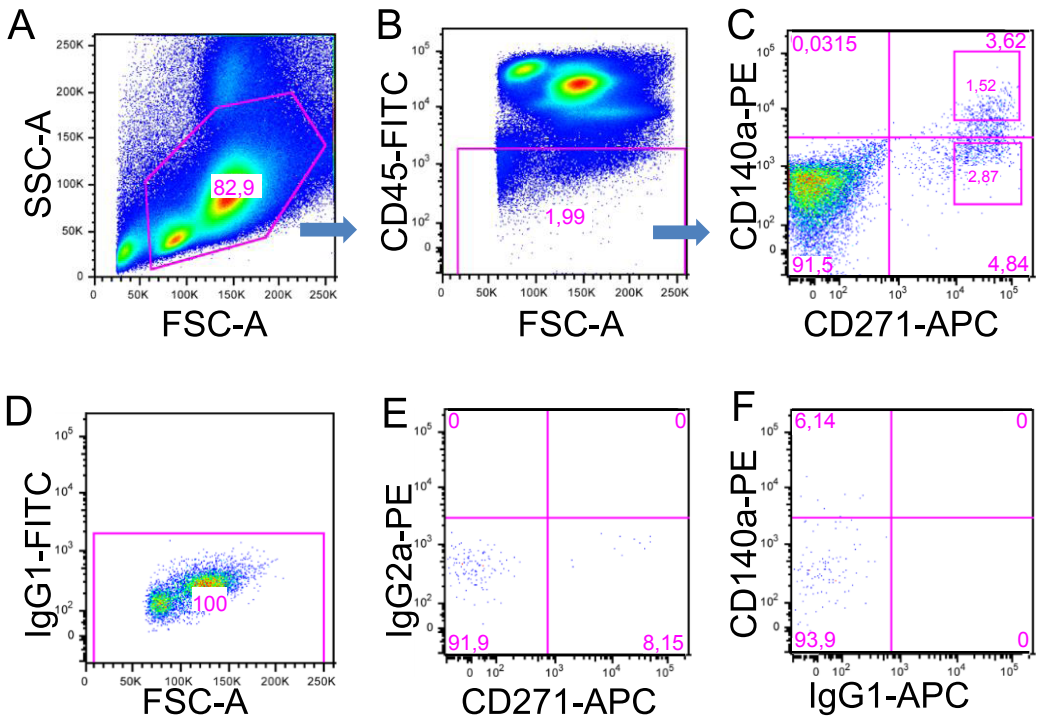
A
SSC-A
FSC-A
82,9
B
CD45-FITC
FSC-A
1,99
C
CD140a-PE
CD271-APC
0,0315
3,62
1,52
2,87
91,5
4,84
D
IgG1-FITC
FSC-A
100
E
IgG2a-PE
CD271-APC
0
0
91,9
8,15
F
CD140a-PE
IgG1-APC
6,14
0
93,9
0

Figure S4

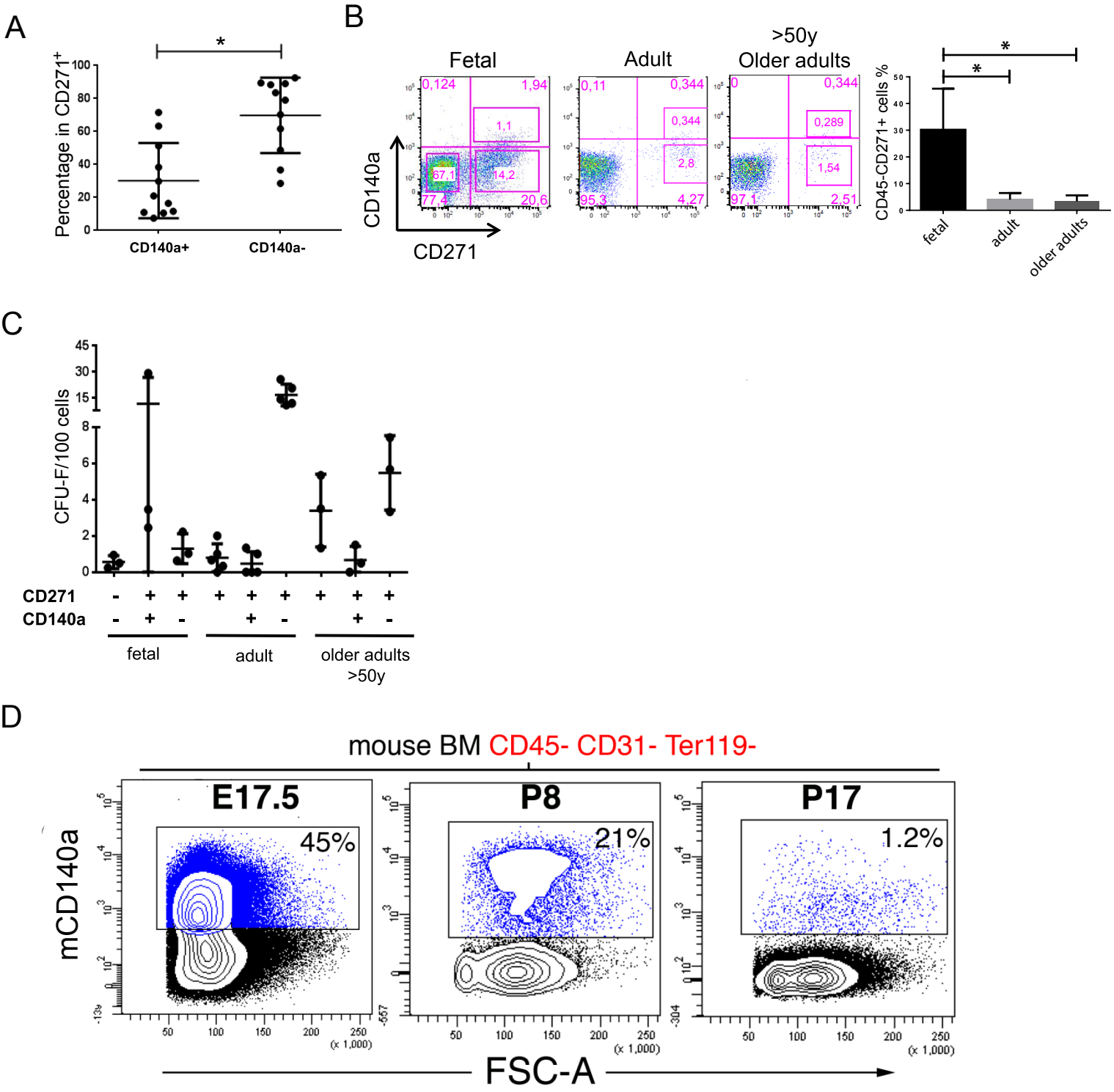
A
Percentage in CD271+
CD140a+
CD140a-
B
Fetal
Adult
>50y
Older adults
CD140a
CD271
0,124
1,94
1,1
67,1
14,2
77,4
20,6
0,11
0,344
0,344
2,8
95,3
4,27
0
0,344
0,289
1,54
97,1
2,51
CD45-CD271+ cells %
fetal
adult
older adults
C
CFU-F/100 cells
CD271
CD140a
fetal
adult
older adults
>50y
D
mouse BM CD45- CD31- Ter119-
E17.5
45%
P8
21%
P17
1.2%
mCD140a
FSC-A
(x 1,000)

Supplemental Figure Legends

Figure S1, related to Figure 1. Gating strategy of isolating lin$^-$/CD45$^-$/CD271$^+$ and lin$^-$/CD45$^-$/CD271$^-$ MNCs for microarray analysis.

Freshly isolated lineage-depleted human BM-MNCs were stained with antibodies against CD271 and CD45 and lin$^-$/CD45$^-$/CD271$^+$ and lin$^-$/CD45$^-$/CD271$^-$ were sorted by FACS following (A) forward/side scatter gating, doublet and dead cell exclusion (7-AAD gating), and gating on CD45$^-$ cells (B). (C) Dot plot illustrating the sorting gates for CD271 expressing cells (upper gate) versus CD271$^-$ cells (C, lower gate). Gates for the CD45/CD271 sorts from lineage-depleted bone marrow were set according to the corresponding fluorescence-minus-one (FMO) control for CD45 (D) and CD271 (E). The figure shows a representative set of FACS plots.

Figure S2, related to Figure 1. MSC properties of lin$^-$/CD45$^-$/CD271$^+$/CD151$^+$ cells and lin$^-$/CD45$^-$/CD271$^+$/LEPR$^+$ cells.

(A) CFU-F frequencies of primary lin$^-$/CD45$^-$/CD271$^+$ bone marrow cell populations sorted on CD151 expression (left plot). Data are presented as individual data (dots) from bulk sorting (right figure, n= 4 independent experiments with at least three replicates for each experiment). (B) Cytospin preparation illustrating the morphology of CD45$^-$/CD271$^+$/CD151$^+$ cells (May-Grünwald/Giemsa staining). Scale bar indicates 20 µm. (C) Quantitative real-time PCR was performed on sorted lin$^-$/CD45$^-$/CD271$^-$/CD151$^-$, lin-/CD45$^-$/CD271$^+$/CD151$^+$, and lin$^-$/CD45$^-$/CD271$^-$/CD151$^+$ cells. Results are shown as fold mRNA change after standardizing with GAPDH levels. Data are given as mean ± standard deviation (SD) from 3 independent experiments. *:$p< 0.05$. (D) Flow cytometric analysis of cultured CD45$^-$/CD271$^+$/CD151$^+$-derived stroma cells stained with typical MSC markers (blue line). Red open histograms represent corresponding isotype controls. One representative set of histograms of a total of three experiments is shown. (E) Multicolor FACS analysis of primary, lineage-depleted BM-MNC after gating on CD45 negative cells. Events are plotted for CD271 (x-axis) against CD151 (y-axis). Red events in the plots indicate cells that co-expressed the marker listed on top of the plot, i.e. CD105, CD90, CD140b, STRO-1, CD31, CD34, SSEA4, and CD34, respectively. Grey events represent cells that did not co-express the listed marker. One representative set of FACS plots of a total of 3 experiments is shown. (F) *In vitro* differentiation capacity of cultured stromal cells generated from CD45$^-$/CD271$^+$/CD151$^+$ cells. Cultured cells were differentiated toward the osteoblastic, adipogenic, and chondrogenic lineage (upper panel). Chondrocyte control sections were stained with the secondary antibody only (lower panel). Scale bars indicate 500 µm (osteoblast), 100µm (adipocyte) and 200 µm (chondrocyte). Representative pictures from one of a total of 3 experiments are shown. (G) Multiclonal cultures generated from CD45$^-$/CD271$^+$/CD151$^+$ cells were transplanted subcutaneously (with HA/TCP particles) into immunodeficient mice. Representative sections 8 weeks after transplantation are shown. Bone (b), adipocytes (a), fibroblastic tissue (ft), and capillaries (*) are indicated. Dark brown areas indicate HA/TCP carrier particles

(magnification 10×). The arrow indicates invading hematopoietic cells. Scale bars indicate 100 µm. (H) Immunostaining of implants with antibodies against mouse CD45 and human vimentin. HA/TCP particles (with or without multiclonal cultures generated from $lin^-/CD45^-/CD271^+/CD151^+$ cells) were transplanted subcutaneously into immunodeficient mice. Representative sections 8 weeks after transplantation are shown. Bone (b), fibroblastic tissue (ft), capillaries (*) and HA/TCP particles are indicated. Dark brown dots indicate cells which were positive for mCD45 or hVimentin (magnification 10×). The empty control implant without MSC is negative for hVimentin and lacks bone formation. Scale bars indicate 100 µm. Sections of implants labeled for anti-mouse CD31 antibody and counterstained with hematoxylin. Scale bars indicate 250 µm (left). Vessel density is expressed as percentage of CD31 positive area relative to the total area of the implant (right). Data are shown as mean ± SD of three to six independent experiments, *:$p< 0.05$. (J) FACS plot showing the expression of LEPR in primary $lin^-/CD45^-/CD271^+/CD140a^-$ bone marrow cells in adult donors (left). Percentages of LEPR positive and negative cells in the $CD45^-/CD271^+/CD140a^-$ fraction (second from left). CFU-F frequencies of sorted LEPR positive compared to LEPR negative cells (second from right). Distribution of total colonies between LEPR positive and negative cells (right). Data are shown as mean ± SD of 3 independent experiments, *:$p< 0.05$.

Figure S3, related to Figure 2. Gating strategy for sorting of $lin^-/CD45^-/CD271^+/CD140a^+$ and $lin^-/CD45^-/CD271^+/CD140a^{low/-}$ MNC.

Freshly isolated lineage-depleted human BM-MNCs were stained with antibodies against CD271, CD45, and CD140a and $lin^-/CD45^-/CD271^+/CD140a^+$ and $lin^-/CD45^-/CD271^+/CD140a^{low/-}$ cells were sorted by FACS following (A) forward/side scatter gating (upper row, left plot) and (B) gating on $CD45^-$ cells . Gates for the CD45/CD271/CD140a sorts from lineage-depleted bone marrow were set according to the corresponding FMO controls for CD45 (D), CD140a (E), and CD271 (F). A representative set of FACS plots is shown.

Figure S4, related to Figure 2. CD140a expression on CFU-F in adult, fetal and older adult BM, and CD140a expression of murine non-hematopoietic BM cells over time.

(A) Percentage of $CD140a^+$ and $CD140a^-$ cells in $lin^-/CD45^-/CD271^+$ cells. Data are obtained from 11 independent experiments. *:$p< 0.05$. (B) FACS plots showing the expression of CD271 and CD140a in primary $lin^-/CD45^-$ bone marrow cell populations in fetal, adult and older donors. Human fetal BM sample, between 15-17 embryonic developmental weeks, were obtained from Novogenix Laboratories. Lower limbs were dissected and bone marrow cells were flushed with PBS containing 10% FBS and 1% AB/AM. Bones were crushed and rinsed with PBS to harvest the cells attached to the bone. After 1x Pharm Lyse™ treatment, BM cells were incubated with blocking buffer followed by FACS. In contrast to adult and older adult bone marrows, fetal bone marrow showed a higher percentage of $CD271^+$ cells (right plot). Data are obtained from 4 fetal, 4 adult and 3 elderly bone marrows. *:$p< 0.05$. (C) CFU-

F frequencies of primary $lin^-/CD45^-/CD271^+$, $lin^-/CD45^-/CD271^+/CD140a^+$, $lin^-/CD45^-/CD271^+/CD140a^-$, $lin^-/CD45^-/CD271^-/CD140a^-$ bone marrow cell from fetal, adult and older donors. In contrast to adult marrow, CFU-F were not only detected in $CD271^+$ cells, but also in the $CD271^-$ fraction. Data are presented as individual data (dots) from bulk sorting (n= 3-5 independent experiments). (D) Collagenase-digested mouse bone marrow samples from the indicated fetal and postnatal stages were stained with antibodies against mouse CD45, CD31, Ter119, CD140a and subjected to FACS analysis. Note the progressive down-regulation and the decrease of the stromal fraction expressing CD140a during postnatal times. In accordance with previously published data (Takashima et al., 2007), we found that the fraction of CD140a expressing cells in murine $CD45^-/CD31^-/TER119^-$ BM cells decreased from 45% at E17.5 (embryo day 17.5) to 21% at P8 (postnatal day 8) and 1.2% at P17. A representative set of FACS plots with the corresponding $CD140a^+$ frequency (within all stromal population), at each stage is shown. Primary anti-mouse antibodies used to stain murine BM samples were the following (all from BD Biosciences): CD45-biotin (clone 30-F11), CD31-biotin (clone MEC13.3), Ter119-biotin (clone TER-119) and CD140a-APC (clone APA5). For CD140a staining, murine bones were dissected at different stages, gently crushed and digested with collagenase type I (Stem cell technologies). Samples were stained with the aforementioned antibodies and mBMSC cells identified by negative gating on $CD45^-/CD31^-/Ter119^-$ population.

Table S2, related to Figure 1. Up-regulated surface marker genes in lin$^-$CD45$^-$CD271$^+$ cells

Gene name and description	Fold change*
VCAM1/CD106 : vascular cell adhesion molecule 1	52.23
ITGB5 : integrin beta-5	41.91
IL11RA : interleukin 11 receptor, alpha	27.62
GHR: growth hormone receptor	16.08
LEPR/CD295 : leptin receptor	15.40
PDGFRB/CD140b : beta-type platelet-derived growth factor receptor	14.60
CDH11: cadherin-11	14.45
CD81 : tetraspanin-28 (Tspan-28)	13.66
FGFR3/CD333 : fibroblast growth factor receptor 3	11.02
PDGFRA/CD140a: alpha-type platelet-derived growth factor receptor	10.93
TNFRSF19 : tumor necrosis factor receptor superfamily, member 19	8.74
TGFBR2 : transforming growth factor, beta receptor II	7.48
TNFRSF1A : tumor necrosis factor receptor superfamily member 1A	6.95
TMEM98 : transmembrane protein 98	6.77
TMEM119 : transmembrane protein 119	6.22
ITGB2/CD18 : integrin beta-2	6.10
IFNGR2 : interferon gamma receptor 2	5.90
CNTNAP2 : contactin-associated protein-like 2	5.74
ABCA8 : ATP-binding cassette sub-family A member 8	5.57
IL1R1 : interleukin 1 receptor, type I	4.84
TGFBR3 : transforming growth factor beta receptor III	4.61
CD151 : a member of the tetraspanin family	4.52
MME/CD10 : membrane metallo-endopeptidase, neprilysin	3.97
NTRK2 : neurotrophic tyrosine kinase, receptor, type 2	3.92
TMEM2 : transmembrane protein 2	3.75
BST2/CD317 : tetherin, bone marrow stromal antigen 2	3.61
FCRLA : Fc receptor-like A	3.13
EFNA1: Ephrin-A1	3.10

* Fold change represents the differences of the mean gene expression intensity in lin$^-$/CD45$^-$/CD271$^+$ compared to lin$^-$/CD45$^-$/CD271$^-$ cells. Gene expression analysis was performed on sorted cells from five donors.

Table S3, related to Figure 1-3. Primer sequences for qRT-PCR analysis*

GAPDH	F	5'- CACTCCACCTTTGACGC -3'
	R	5'- GGTCCAGGGGTCTTACTCC -3'
ACAN	F	5'- ACTCTGGGTTTTCGTGACTCT -3'
	R	5'- ACACTCAGCGAGTTGTCATGG -3'
ALPL	F	5'- AGCTGAACAGGAACAACGTG -3'
	R	5'- CAGCAAGAAGAAGCCTTTGG -3'
CD45	F	5'- ACCTTGAACCCGAACATGAG -3'
	R	5'- TCCTGGACTCCCAAAATCTG -3'
CD81	F	5'- TAACACGTCGCCTTCAACTG -3'
	R	5'- GAAGGAACATCAGGCATGCT -3'
CD151	F	5'- TCATCCTGCTCCTCATCATC -3'
	R	5'- TTGGTCATGGTGTCCTTCAG -3'
CD271	F	5'- CTGCAAGCAGAACAAGCAAG -3'
	R	5'- TCGCTGTGGAGTTTTTCTCC -3'
LEPR	F	5'- ACCTCTGGTTCCCCAAAAAG -3'
	R	5'- GTCGTTGAGTTTGGCTGTTG -3'
Nanog	F	5'- AACAATCAGGCCTGGAACAG -3'
	R	5'- GAGAATTTGGCTGGAACTGC -3'
Oct4	F	5'- GAGGATTTTGAGGCTGCTG -3'
	R	5'- TAGCCTGGGGTACCAAAATG -3'
PPARg	F	5'- TGCAGGTGATCAAGAAGACG -3'
	R	5'- GAAGGGAAATGTTGGCAGTG -3'
Sox-2	F	5'- AGAACCCCAAGATGCACAAC -3'
	R	5'- CGTCTCCGACAAAAGTTTCC -3'
VCAM1	F	5'- TCCGTCTCATTGACTTGCAG -3'
	R	5'- CATTCGTCACCTTCCCATTC -3'
CXCL12	F	5'- TGCCGATTCTTCGAAAGC -3'
	R	5'- ATCTGAAGGGCACAGTTTGG -3'
ANGPT1	F	5'- TCACATAGGGTGCAGCAATC -3'
	R	5'- ACAGTTGCCATCGTGTTCTG -3'
SPP1	F	5'- GAAGTTTCGCAGACCTGACAT -3'
	R	5'- GTATGCACCATTCAACTCCTCG -3'
DcR2	F	5'-TACCACGACCAGAGACACC -3'
	R	5'-CACCCTGTTCTACACGTCCG -3'
p21	F	5'-TGAGCCGCGACTGTGATG -3'
	R	5'- GTCTCGGTGACAAAGTCGAAGTT -3'
p16	F	5'- ATGGAGCCTTCGGCTGACT -3'
	R	5'- GTAACTATTCGGTGCGTTGGG -3'

*All primers were obtained from Life Technologies.

Supplemental Experimental Procedures

Antibodies

For FACS analysis and cell sorting the following antibodies were used: CD31-FITC (clone WM59), CD34-FITC (clone 581), CD45-FITC (clone 2D1), CD90-FITC (clone 5E10), HLA-DR-FITC (clone L243), SSEA4-FITC (clone MC813-70), CD10-PE (clone HI10a), CD14-PE (clone MϕP9), CD18-PE (clone 6.7), CD19-PE (clone SJ25C1), CD34-PE (clone 8G12), CD45-PE (clone HI30), CD73-PE (clone AD2), CD81-PE (clone JS-81), CD106-PE (clone 51-10C9), CD140a-PE (clone αR1), CD151-PE (clone 14A2.H1), CD166-PE (clone 3A6), HLA-ABC-PE (clone G46-2.6), CD106-APC (clone 51-10C9), CD45-APC-Cy7 (clone 2D1), purified GD2 (clone 14.G2a) (all from BD Bioscience, Erembodegem, Belgium), CD271-FITC, CD271-PE, CD271-APC (clone ME20.4-1.H4, Miltenyi Biotec, Bergisch Gladbach, Germany), purified STRO-1 (clone STRO-1), TGFBRII-PE (clone 25508), TGFBRIII-PE, FGFR3-PE (clone 136334), IFNGR2-APC, IL1R1-PE, TNFR1-PE (clone 16803), LEPR-PE (clone 52263) (all from R&D Systems, Abingdon, United Kingdom), CD105-FITC (clone SN6, AbD Serotec, Kidlington, UK), and PDGFR-beta-FITC (clone 7H36, US Biological, Swampscott, MA, USA). Matching isotype controls were from BD Bioscience and R&D Systems. For unconjgated primary antiobodies, goat anti-mouse IgG2a-FITC and goat anti-mouse IgM-FITC (Jackson ImmunoResearch Laboratories, Inc., Suffolk, UK) were used as secondary antibodies. For staining of cryo sections antibody against aggrecan was used followed by secondary antibody staining (donkey anti-goat IgG-Texas Red, Jackson ImmunoResearch Laboratories).

Microarray expression analysis

RNA from sorted cell populations was isolated, subjected to a two-round amplification and analyzed for gene expression by microarray analysis using Illumina Human HT-12 expression v4 BeadChips (Illumina, San Diego, CA). Pre-hybridization treatment, hybridization and post-hybridization washes were performed using the Illumina hybridization protocol (Manual 11322187 Revision A). Basic Illumina chip and Experimental Quality Analyses were performed using the GenomeStudio software V2011.1. 2. Probe summarization and data normalization were performed as described previously (Tusher et al., 2001). Signals were log2 transformed after probesets having no gene annotations or expired annotations were filtered out. SAM (significance analysis of microarrays) analysis was performed to identify significantly differentially expressed genes between groups following quantile normalization in the BioArray Software Environment (BASE). SAM was performed with Delta = 15.321 pursuing a false positive rate of 0%. Normalized data have been deposited in the GEO database (GSE57927).

Flow cytometry

Cultured cells were harvested, washed, and unspecific binding was blocked with human normal immunoglobulin. Cells were stained (30 min, 4˚C) with combinations of antibodies and samples were analyzed on a FACS Calibur (BD). Freshly isolated RosetteSep-depleted BM-MNCs were antibody stained (see Supplementary Materials) and analyzed on a LSR II flow cytometer (BD).

CFU-F assay and limiting dilution assay

FACS-sorted cells were cultured at plating densities of 1-10 cells/cm^2 when assaying CD45$^-$/CD271$^+$/CD151$^+$, CD45$^-$/CD271$^+$/CD140a$^{low/-}$ and CD45$^-$/CD271$^+$/CD140a$^+$ sorted cells, and 1000 cells/cm^2 in case of lineage-depleted unsorted cells. Colonies were counted after 14 days

(1% Crystal Violet, Sigma). Colonies containing ≥40 cells were counted as CFU-F. Generally, assays were set up in duplicates or triplicates.

For single cell CFU-F assays, cells were sorted into 96-well plates and cultured in MSC medium. Colonies were counted after 3 weeks, harvested and split for continued culture for in vitro differentiation assays.

Limiting dilution assays were performed with $CD271^{+}/CD45^{-}/CD140a^{low/-}$ cells seeded at plating densities of 1, 2, 3, 4, 5, 10 and 20 cells per well in 96-well plate in replicates of 8 wells per density level. Colony frequencies were calculated using Poisson distribution statistics (L-CalcTM software, StemCell Technologies).

Cell cycle analysis

BM mononuclear cells were stained with antibodies against CD45, CD271, and CD140a followed by fixation/permeabilization (Cytofix/Cytoperm kit, BD Biosciences) and intracellular staining with anti-KI67-FITC (BD) and DAPI (Sigma). Analysis was performed on a LSR II flow cytometer (BD).

***In vitro* differentiation assays – differentiation-induction media**

Osteogenesis induction medium contained of NH Expansion medium (Miltenyi Biotec), 1% Antibiotic/Antimicotic solution, 10 mM β-glycerophosphate, 0.1µM Dexamethasone (all from Sigma), 0.05 mM L-ascorbic acid (Wako chemicals, Richmond, VA, USA)]. Chondrogenesis-induction medium contained of DMEM-high glucose supplemented with 0.1 µM dexamethasone, 1 mM sodium pyruvate, 0.35 mM L-proline (all from Sigma), 0.17 mM ascorbic acid (Wako Chemicals, Richmond, VA, USA), 1% ITS+ culture supplements (BD Biosciences) and 0.01 µg/ml TGF-ß3 (R&D Systems, Abingdon, UK)].

Quantitative real-time PCR

RNA was isolated using QIAshredder Homogenizers columns (Qiagen) and RNeasy Micro Kit (Qiagen) according to the manufacturer's protocol. The concentration and purity of RNA was determined by Nanodrop (Thermo Fisher Scientific, Gothenburg, Sweden). cDNA was synthesized using SuperScript VILO cDNA synthesis kit (Life Technologies) on C1000^{TM} Thermal Cycler (Bio-Rad, Hercules, CA, USA). Quantitative real-time PCR analysis was carried out using Fast SYBR master mix (Applied Biosystems by Life Technologies) according to manufacturer's instructions. Primer sequences are listed in Table S3. The crossing point of each sample was measured and analyzed with StepOne Software v2.1 (Applied Biosystems). Each gene-specific mRNA was normalized to the housekeeping gene Glyceraldehyde 3-phosphate dehydrogenase (*GAPDH*) mRNA. The expression of each mRNA was determined using the $2^{-\Delta\Delta CT}$ threshold cycle method.

Immunohistochemistry and quantification of CD31-pos vasculature

Paraffin sections of implants were stained for CD31 (ab28364, Abcam) using standard immunohistochemistry methods, developed with DAB and counterstained with hematoxylin. Positive staining appeared as brown precipitate associated to vascular structures. High-resolution images of CD31-stained sections were acquired using a digital slide scanner (Hamamatsu), encompassing the whole implant. Digital images were processed using Image J analysis software (NIH). For calculation of the CD31-positive vasculature area, DAB-stained areas were measured after color deconvolution by adjusting the threshold levels in the brown component channel. Vessel density was expressed as percentage of $CD31^+$ area relative to the total implant tissue area.

Supplemental References

Takashima, Y., Era, T., Nakao, K., Kondo, S., Kasuga, M., Smith, A.G., and Nishikawa, S. (2007). Neuroepithelial cells supply an initial transient wave of MSC differentiation. Cell *129*, 1377-1388.

Tusher, V.G., Tibshirani, R., and Chu, G. (2001). Significance analysis of microarrays applied to the ionizing radiation response. Proc Natl Acad Sci U S A *98*, 5116-5121.